

# Nucleoplasmic Organization of Small Nuclear Ribonucleoproteins in Cultured Human Cells

A. Gregory Matera and David C. Ward

Departments of Genetics and Molecular Biophysics and Biochemistry, Yale University School of Medicine, New Haven, Connecticut 06510

**Abstract.** The organization of eight small nuclear ribonucleoproteins (the U1, U2, U4, U5, and U6 RNAs previously studied by others and three additional snRNAs, U11, U12, and 7SK) has been investigated in cultured human cells by fluorescence in situ hybridization with antisense DNA and 2'-O-Me RNA oligonucleotides. Using highly sensitive digital imaging microscopy we demonstrate that all of these snRNAs are widespread throughout the nucleoplasm, but they are excluded from the nucleoli. In addition, the U2, U4, U5, U6, and U12 snRNAs are concentrated in discrete nuclear foci, known as coiled bodies, but U1 and 7SK are not. In addition to coiled bodies, a classic

speckled pattern was observed in the nucleoplasm of monolayer-grown HeLa cells, whereas suspension-grown HeLa cells revealed a more diffuse nucleoplasmic labeling. Immunofluorescence staining using various snRNP-specific antisera shows complete agreement with that of their antisense snRNA oligonucleotide counterparts. Although U2 RNA is concentrated in coiled bodies, quantitation of the fluorescence signals from the U2 antisense probe reveals that the bulk of the U2 snRNP is located in the nucleoplasm. Furthermore, simultaneous visualization of the U2 snRNAs and the tandemly repeated U2 genes demonstrates that coiled bodies are not the sites of U2 transcription.

**S**MALL nuclear ribonucleoproteins (snRNPs)<sup>1</sup> have been shown to play key roles in RNA processing reactions that form a vital link in the pathway of gene expression (for reviews see Steitz et al., 1988; Reddy and Busch, 1988). Pre-mRNA splicing is directed within a large multi-snRNP complex called the spliceosome (for review see Green, 1991; Guthrie, 1991). This structure is composed of the U1, U2, U4/U6, and U5 snRNPs and various associated proteins. However, the integration of the splicing machinery within the architecture of the mammalian nucleus is at present poorly understood. Studies of amphibian oocytes show that the relatively large nuclear organelles known as spheres contain snRNPs (Gall and Callan, 1989). In addition to the larger spheres found in amphibian germinal vesicles, thousands of smaller snRNP-containing granules called snurposomes have also been detected (Wu et al., 1991; Callan and Gall, 1991; Gall, 1991). With the exception of nucleoli, however, the functions of these extrachromosomal domains are largely a matter of speculation.

Nuclear substructures called accessory bodies were first identified in 1903 using the light microscope (Ramon y

Cajal, 1903). These same organelles were later observed in the electron microscope and termed coiled bodies (Hardin et al., 1969; Monneron and Bernhard, 1969; Seite et al., 1982; Lafarga et al., 1983) due to their coiled fibrillar appearance. In addition to nucleoplasmic staining (of perichromatin fibrils and interchromatin granules), coiled bodies (CBs) were also detected in rat and mouse liver thin sections using anti-Sm antibodies (Fakan et al., 1984). Immunoelectron (Elicieri and Ryerse, 1984) and immunofluorescence (Leser et al., 1989) analyses of HeLa cells revealed the existence of intranuclear clusters of Sm protein epitopes. These clusters were then identified as CBs using a novel class of autoimmune antisera (Raska et al., 1990, 1991) which specifically recognize an 80-kD protein within CBs called p80 coilin (Andrade et al., 1991). The pattern of intranuclear localization appears to be remarkably dependent on the cell type, growth conditions, and the nature of the probe as well as on the fixation and hybridization conditions.

Curiously, previous light microscopic studies of mammalian nuclei using antibodies specific for spliceosomal snRNP proteins revealed a nucleoplasmic speckled staining pattern in which CBs were not detected (Spector, 1984, 1990; Nyman et al., 1986; Verheijen et al., 1986). Using novel, highly specific antisense 2'-O-methyl (2'-OMe) RNA oligonucleotide probes, two laboratories have recently investigated the distribution of the most abundant snRNAs (Carmo-Fonseca et al., 1991a,b, 1992; Huang and Spector, 1992). Both groups agree that HeLa cells contain clusters or

Please address all correspondence to Dr. A. G. Matera, Department of Genetics, Yale University School of Medicine, 333 Cedar Street, New Haven, CT 06510.

1. *Abbreviations used in this paper:* CBs, coiled bodies; CCD, charge-coupled device; 2'-OMe, 2'-O-methyl; snRNPs, small nuclear ribonucleoproteins.

foci which are enriched in snRNA complexes in addition to nucleoplasmic labeling. Initially, Carmo-Fonseca et al. (1991a,b) showed that U1 was widely dispersed throughout the nucleoplasm, but that U2, U4, U5, and U6 snRNAs were detected only in foci (even though antibodies to U2 proteins revealed additional nucleoplasmic staining). Later, they identified the snRNP-rich foci as coiled bodies and demonstrated a more complete colocalization of the RNA and protein components of the U2 snRNP (Carmo-Fonseca et al., 1992). Huang and Spector (1992) have found that U1 and U2 colocalize in both CBs and nuclear speckles. The speckled pattern, however, was only detected after a lengthy period of hybridization. Additionally, Spector et al. (Huang and Spector, 1992; Spector et al., 1992) report that CBs are not observed in cell lines of defined passage, a finding which may explain why coiled bodies were not detected in previous immunofluorescence studies.

The studies mentioned above have demonstrated the existence of snRNP-rich structures within mammalian nuclei using antisense 2'-OMe RNA oligonucleotide probes. Double labeling experiments with antisense RNA probes and antibodies specific to snRNP proteins showed that the two components colocalized in the case of the U1 snRNPs, whereas the U2 antisense probe recognized only a subset of the anti-U2 antibody staining pattern. Here we present a reinvestigation of the organization of the five (U1, U2, U4, U5, and U6) spliceosomal RNAs as well as three other snRNAs (U11, U12, and 7SK) using a highly sensitive cooled charge-coupled device (CCD) digital imaging system that also permits the quantitation of the distribution of snRNAs in the nucleus.

## Materials and Methods

### Oligonucleotide Synthesis and Labeling

Amine-modified DNA and 2'-OMe RNA oligonucleotides were used to create antisense snRNA probes. The sequences were chosen on the basis of their specificity in RNase H-targeted digestion and 2'-OMe selection of snRNP particles (Blencowe et al., 1989; Carmo-Fonseca et al., 1991a; Wassarman and Steitz, 1991; Montzka Wassarman and Steitz, 1992). The oligonucleotides were synthesized using a DNA synthesizer (Applied Biosystems Inc., Foster City, CA). Primary amine functionalities were introduced at specific T residues using Amino-modifier-dT (Glen Res. Corp., Sterling, VA). This phosphoramidite provides a primary amine, coupled through a 12-atom spacer arm, which can then be labeled by a variety of haptens or fluorophores. Table I provides detailed information about the oligonucleotides used in this study. Two identical anti-U2 oligomers were synthesized in parallel (see Table I), one of which was phosphorothiolated at each residue, after the method of Iyer et al. (1990). Unlabeled anti-U2 and various other biotinylated 2'-OMe RNA oligonucleotides (see Table I) were obtained from the laboratory of Dr. J. Steitz. Digoxigenin and fluorescein labeling of both DNA and 2'-OMe RNA oligomers was performed as described previously (Matera and Ward, 1992).

### Cell Culture

HeLa-JS1000 cells were grown in spinner flasks in DMEM and supplemented with 10% FBS and antibiotics. The cultures were divided and fed daily. A monolayer HeLa line (called here HeLa-ATCC) was also grown on chambered microscope slides (Nunc, Naperville, IL) in the same medium. Additional experiments were performed on three B-lymphoblastoid cell lines (Raji, BJAB-B1, and BJAB) and one breast cancer cell line (MCF-7). The B-cell lines were grown in suspension as described in Toczycki and Steitz (1991). The MCF-7 cells were grown as monolayers on slides as described (Brown et al., 1984). For antibody screening only, additional experiments were performed using an immunofluorescence antibody kit containing prefixed, dried human epithelial (HEp-2) cells (Quidel, San Diego, CA).

### Slide Preparation

Before fixation, 5 ml ( $\sim 10^6$  cells) of HeLa-JS1000 were removed from culture, spun down in a clinical centrifuge and resuspended in 10 ml of 1× PBS, 2 mM MgCl<sub>2</sub>. The cells (0.5 ml/slide) were spun onto Vectabond (Vector Labs, Inc., Burlingame, CA) treated slides in a Cytospin2 (Shandon Inc., Pittsburgh, PA) cytofuuge at 750 rpm for 5 min, and then were fixed for 10 min in 1× Fixation buffer (4% paraformaldehyde, 100 mM KCl, 20 mM NaPipes-pH 7.4, 15 mM  $\beta$ -mercapto-ethanol, 2.5 mM MgCl<sub>2</sub>, 0.5 mM EGTA) at room temperature. The slides were then quenched in 100 mM glycine, PBS for 5 min, and rinsed in PBS before permeabilization in  $-20^{\circ}\text{C}$  acetone for 5 min. After three washes in PBS, the slides were stored in PBS at  $4^{\circ}\text{C}$  for up to 1 wk. The cells that were grown in chambered slides were aspirated to remove the medium, rinsed in PBS, and then fixed and permeabilized as described above. Several additional fixation/extraction conditions were also tested: (a) Preextraction in 0.5% Triton X-100, 0.5 × PBS, 5 mM MgCl<sub>2</sub> for 1 min at  $0^{\circ}\text{C}$  followed by fixation in 4% paraformaldehyde in either PBS or the Fixation buffer described above. (b) Fixation in 4% paraformaldehyde (buffered with PBS, 1× Fixation buffer or CSK buffer [100 mM NaCl, 10 mM Pipes-pH 6.8, 300 mM sucrose and 3 mM MgCl<sub>2</sub>]) followed by extraction in either 0.5% Triton X-100, 0.5% saponin, PBS for 5 min at  $0^{\circ}\text{C}$ , or in  $-20^{\circ}\text{C}$  acetone for 5 min. (c) Preextraction with 0.2% NP-40, in 0.5 × PBS at  $0^{\circ}\text{C}$  for 5 min, fixation in 1× Fixation buffer, 4% paraformaldehyde for 10–45 min, and extraction with 0.5% Triton X-100, 0.5% saponin in PBS followed by three cycles of liquid N<sub>2</sub> freeze-thaw using slides equilibrated in 20% glycerol, PBS.

### In Situ Hybridization

Before hybridization, the slides were removed from storage and blocked in 250  $\mu\text{l}$  of 4× SSC, 3% BSA under a 24 × 50-mm coverslip for 20 min at  $37^{\circ}\text{C}$  in a humid chamber. Hybridization was performed in 4× SSC, 10% dextran sulfate containing 1–2 ng/ $\mu\text{l}$  of labeled probe oligomer (1–5 pM) and  $\sim 150$  ng/ $\mu\text{l}$  of a competitor oligonucleotide. The sequence of the competitor oligonucleotide is relatively unimportant; the oligomer used here was an unlabeled, amine-modified 24-mer (5'-CTGGGTTCCTGCCGTCGCG-GTG-3') complementary to the spacer region of a human 5 S rDNA repeat. The hybridization cocktail was prewarmed in a  $37^{\circ}\text{C}$  heat block before 20  $\mu\text{l}$  were applied per slide under a 22 × 22-mm coverslip. The slides were incubated for 20 min at  $37^{\circ}\text{C}$  in a humid chamber, and then were washed (3 × 5 min) in 4× SSC, 0.1% Tween-20 at  $37$ – $42^{\circ}\text{C}$ . After a blocking step in 4× SSC, 3% BSA, 0.1% Tween for 20 min, the probes were detected with FITC- or Texas red-conjugated Avidin-DCS (Vector Labs Inc.) or rhodamine- or fluorescein-conjugated antidigoxigenin F<sub>ab</sub> fragments (Boehringer Mannheim Corp., Indianapolis, IN) and again washed in 4× SSC, 0.1% Tween,  $37^{\circ}\text{C}$  (3 × 5 min). Samples were then counterstained in 4× SSC, 0.1% Tween, 200 ng/ml DAPI (4,6-diamidino-2-phenylindole) (Boehringer Mannheim Corp.) at room temperature, washed again briefly in 4× SSC, 0.1% Tween, and mounted in antifade: 90% glycerol, 0.1 M Tris-pH 8.0 and 2.3% (wt/vol) DABCO (1,4-diazobicyclo-2,2,2-octane) (Sigma Chem. Co., St. Louis, MO).

### Antisense RNA Double Label

The images in Fig. 3 (A–L) were all obtained by first focusing on the CBs in the U2 signal channel. The other two signal channels (the second oligonucleotide and the DNA counterstain) were then imaged in sequence without changing the focus.

### U2 Gene and snRNA Double Label

To visualize specific RNA and DNA sequences in the same experiment, we used a procedure similar to that of Carter et al. (1991). A plasmid clone of the 6-kb human U2 snRNA tandem repeat unit (a gift of A. Weiner) was nick-translated with digoxigenin-dUTP as described in Lichter et al. (1990). Using fixed, undenatured HeLa cells, a biotinylated 2'-OMe anti-U2 oligonucleotide probe was first hybridized, washed, and detected with FITC-Avidin as described above. The slides were then refixed with 4% paraformaldehyde in PBS for 10 min and quenched in 100 mM glycine, PBS for 5 min and again rinsed in PBS. The cells were denatured under a sealed 18 × 18-mm coverslip in 15  $\mu\text{l}$  of a solution of 45% formamide, 2× SSC, 10% dextran sulfate, 80 ng of the U2 gene probe, 3  $\mu\text{g}$  of human C<sub>at</sub> 1 DNA repeat competitor (GIBCO BRL, Gaithersburg, MD) and 8  $\mu\text{g}$  of salmon sperm carrier DNA for 5 min at  $80^{\circ}\text{C}$ . The DNA was allowed to hybridize for 6 h at  $37^{\circ}\text{C}$  in a humid chamber. After washing in 50% formamide, 2× SSC,  $25^{\circ}\text{C}$  (3 × 5 min), and again in 1× SSC,  $55^{\circ}\text{C}$  (3 × 5 min)

the slides were blocked, detected with rhodamine-conjugated antidigoxigenin antibodies, washed, counterstained in DAPI, and mounted in antifade as described above. As in the other double hybridization experiments, signals from the CBs seen with the U2 oligoprobe were used as focusing objects before images were taken in the other filter channels. Hence, all of the U2 gene loci were not always visible in the same focal plane(s) as the coiled bodies.

### Indirect Immunofluorescence

The following anti-snRNP antibodies were used in conjunction with antisense snRNA probes: anti-Sm mouse mAb Y<sub>12</sub> (Lerner et al., 1981), anti-U2 human antisera Ya and Ga, and anti-U1 human serum Do (Craft et al., 1988; Bruzik and Steitz, 1990). Coiled bodies were detected using rabbit  $\alpha$ -p80 coilin (Andrade et al., 1993). Detection of primary antibodies was accomplished using the following secondary antibodies: FITC-conjugated goat anti-mouse IgG, FITC-conjugated goat anti-rabbit IgG (Sigma Chem. Co.), and either FITC- or Texas red-conjugated horse anti-human IgG (Vector Labs Inc.). The Y<sub>12</sub> mAb was simply added to the avidin detection step after blocking with 4 $\times$  SSC, 3% BSA, 0.1% Tween as described above. After washing and a brief blocking step, the secondary antibody was similarly reacted and washed before counterstaining and mounting. Staining with the human and rabbit antisera required reduced stringency treatment (lower salt) than did the Y<sub>12</sub> antibody. After the avidin detection step, the slides were blocked and detected in PBS, 3% BSA, 0.1% Tween (20 min each), and washed in PBS, 0.1% Tween (3 $\times$  5 min) before counterstaining (also in PBS) and mounting.

### Digital Imaging Microscopy

Images were acquired using either a Zeiss Axioskop (63 $\times$ , 1.2 n.a. Plan Neofluar oil immersion objective) epifluorescence microscope fitted with a cooled CCD camera (Photometrics Ltd., Tucson, AZ) or an MRC-600 confocal laser-scanning microscope (BioRad Labs., Hercules, CA). The CCD microscope was equipped with precision filters specific for each fluorophore that limit image displacement to  $\pm 1$  pixel when switching filter channels. For routine image acquisition, the 14-bit source images were saved as normalized 8-bit grayscale data files using a software package called CCD Image Capture (developed by T. Rand in the laboratory of D. C. Ward). For quantitative analysis, the program Nu200 (Photometrics Ltd.) was used, since it retains the full 14-bit grayscale, allowing analysis and comparison of separate images. Merging and 24-bit pseudocoloring was accomplished using Gene Join (T. Rand, Yale University) on a Macintosh IIfx computer. DAPI, FITC (or fluorescein), and rhodamine (or Texas red) images are shown in blue, green, and red, respectively. The images were photographed directly from the computer monitor.

## Results

### In Situ Localization of snRNPs

Previous studies found marked differences in snRNP labeling patterns depending upon which method of cell preparation was used (Carmo-Fonseca et al., 1991a,b). We find no major changes in the observed in situ localization of snRNPs when cells are either preextracted with Triton X-100 and then fixed (Fig. 1, a and b, e and f) or when they are fixed first and then extracted with acetone (Fig. 1, c and d, g and h), or detergents (not shown). Both the biotinylated U2(30–43) antisense oligoprobe (Fig. 1, a–d) and the anti-Sm (Y<sub>12</sub>) antibody probe (Fig. 1, e–h) show CBs and widespread nucleoplasmic labeling, excluding nucleoli. Cells that have been permeabilized (after an aldehyde fixation step) with acetone or methanol are morphologically distinct from cells preextracted with nonionic detergents. Organic solvents such as acetone remove water, as well as extracting lipids, etc., causing a significant decrease in cell height (Bacallao et al., 1989 and Matera, A. G., unpublished observations). We also observe that the nuclei that have been acetone extracted appear flatter and rounder (Fig. 1, compare a and b with c and d). In Triton preextracted HeLa-JS1000 cells, it becomes increas-

ingly difficult to view multiple CBs (even within a single cell) in the same plane of focus. Acetone extraction helps reduce this topological problem, as well as providing a secondary fixation step.

### Organization of Spliceosomal snRNAs

Having established fixation and hybridization conditions for U2 snRNA, the acetone permeabilization procedure was then used in separate experiments to investigate the distribution of the U1, U4, U5, and U6 snRNAs, each identified using antisense probes (see Table I). Fig. 2 (a–d) shows that U1 is widely distributed throughout the nucleoplasm of both suspension (JS1000) and monolayer (ATCC) HeLa cells, but CBs are not observed. Although the ATCC cells showed more of a speckled pattern with the U1 oligoprobe than did the JS1000 cells, there was a substantial amount of diffuse nucleoplasmic labeling. However, the U2 oligoprobe reveals a distinct speckled pattern throughout the nucleoplasm of monolayer ATCC cells (Fig. 2, e and f) in addition to 3–5 coiled bodies. JS1000 cells have only 1–2 CBs (see below) and do not display the speckled nucleoplasmic pattern (Fig. 1, c and d). This same nucleoplasmic labeling of U1 and U2 snRNP persisted even after the JS1000 cells were allowed to adhere to the culture flask and were passaged three times before they were grown on chambered slides for microscopy (data not shown). Thus, the change in growth conditions from suspension to adherent cultures did not alter the snRNP distribution of JS1000 cells.

Control experiments were also performed in parallel to examine the specificity of the observed hybridization patterns. Mock hybridization with only the unlabeled competitor oligonucleotide showed very low intensity, nonspecific signals throughout the nucleus and cytoplasm (not shown). As a negative control, the EBER-1 oligomer (see Table I) also showed only background hybridization (Fig. 2, g and h). This probe is complementary to one of the snRNAs transcribed by Epstein Barr Virus during infection of B-lymphocytes and is known to be absent in HeLa cells (Toczyski and Steitz, 1991). Furthermore, specific competition of the U2 oligonucleotide probe was also achieved using a 150-fold excess of unlabeled U2 oligomer, reducing the signal to background levels (not shown). Lastly, as a negative control for filter bleedthrough, labeled antisense U2 probe was hybridized and detected with either fluorescein- or rhodamine-conjugated avidin. The filter was then switched to the opposite channel and the recorded images demonstrated that proper channel separation was maintained (data not shown). These results were also confirmed by showing that the U1(1–14) and U2(30–43) oligonucleotides give equivalent patterns when analyzed using a confocal microscope (not shown) or when hybridized to three different B-lymphoblastoid cell types (data not shown).

Since the ratio of the signal intensity of CBs to nucleoplasm was highest with the anti-U2 oligonucleotide, double labeling experiments were performed in conjunction with anti-U2 oligomers to ensure that images containing CBs were captured. Four different digoxigenin-labeled anti-U2 oligomers were tested for this purpose (U2[30–43], U2[25–43], U2[29–43], U2-S[29–43], see Table I), all of which gave the same pattern of hybridization in separate experiments. As shown, in HeLa-JS1000 cells (Fig. 3, a–c) the U1 nucleoplasmic signals are distributed like those of U2, but U1 was not detected

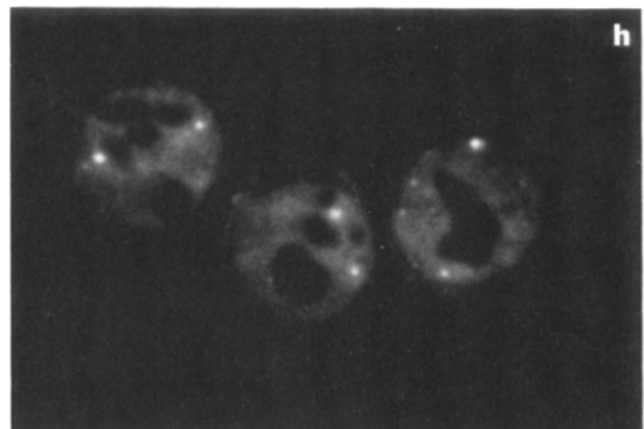
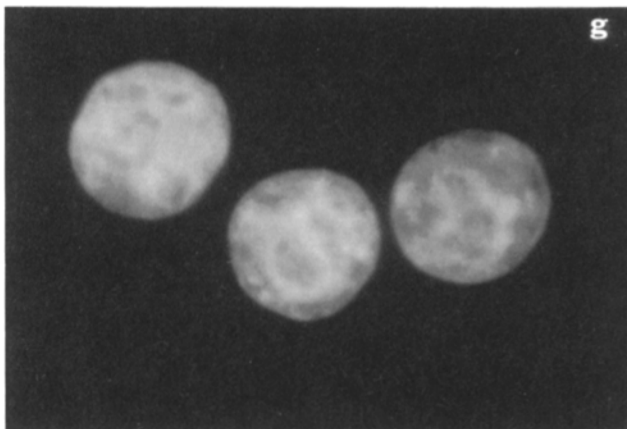
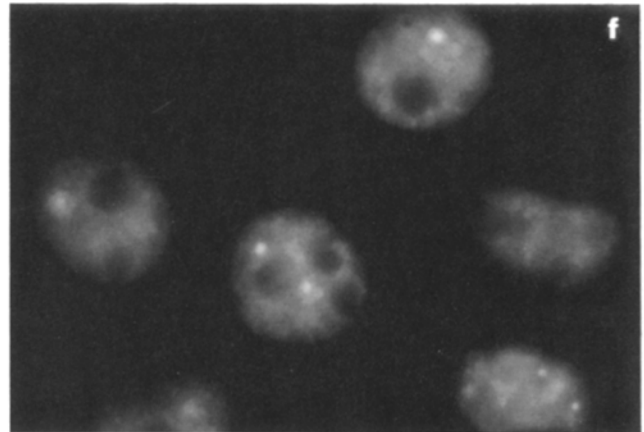
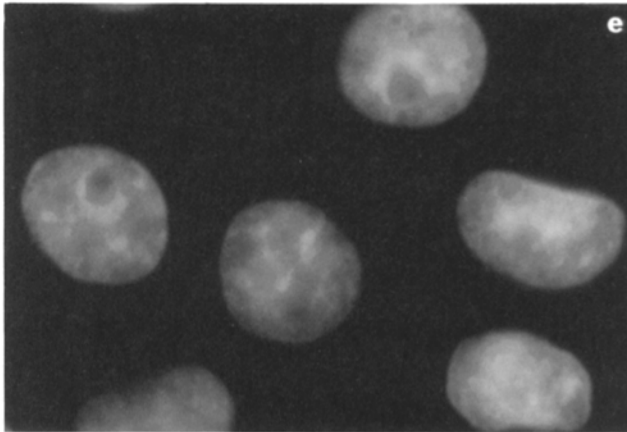
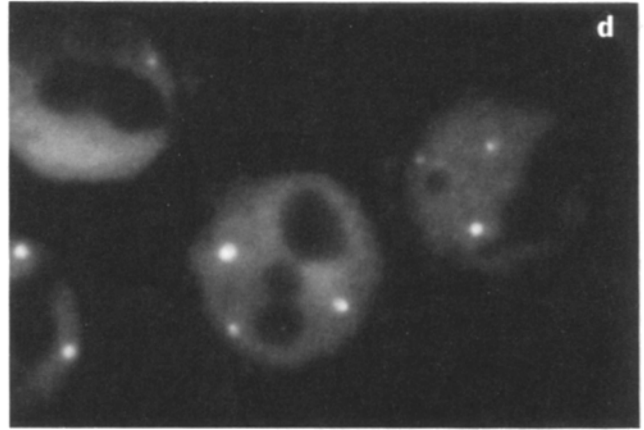
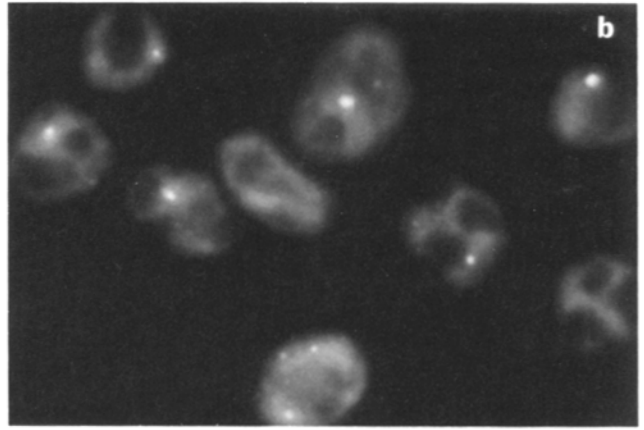
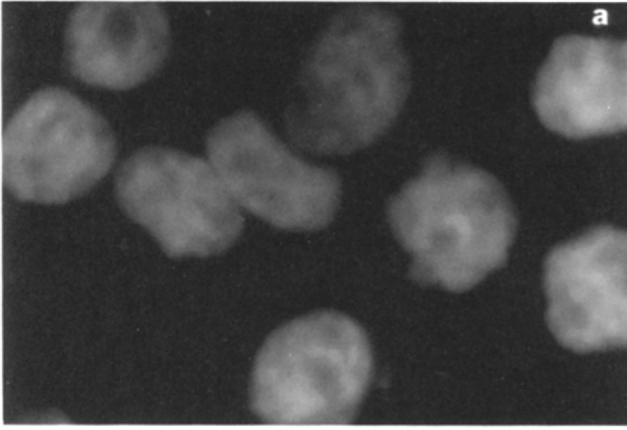


Table I. Oligonucleotide Probes

Target	Sequence	Chemistry	Label(s)	Reference
U1(1-14)	UGCCAGGUAAGUAU(dC*) <sub>4</sub> dA	2'-OMe	Bio	Carmo-Fonseca et al., 1992
U1(1-14)	UGCCAGGUAAGUAU(B) <sub>4</sub> U	2'-OMe	Bio	—
U2(30-43)	ACAIAUACUACACU(dC*) <sub>4</sub> dT	2'-OMe	Bio, Dig	Wassarman and Steitz, 1991
U2(25-43)	ACAGAT*ACT*ACACT*TGAT*C	DNA	Dig, Flu	—
U2(29-43)	ACAGAT*ACT*ACACT*T	DNA	Dig	—
U2-S(29-43)	ACAGAT*ACT*ACACT*T	S-DNA	Dig	—
U4(1-20)	(dC*) <sub>4</sub> UACUICACUICICAAAICU	2'-OMe	Bio	Blencowe et al., 1989; Carmo-Fonseca et al., 1992
U5(36-46)	U(B) <sub>4</sub> UAGUAAAAGGCG(B) <sub>4</sub> U	2'-OMe	Bio	—
U6(81-101)	AT*GGAACGCT*TCACGAAT*TT*G	DNA	Dig	—
U6(57-74)	(dC*) <sub>4</sub> AUCCUUCICAIIIICCA	2'-OMe	Bio	Blencowe et al., 1989
U6(21-40)	AT*CGT*TCCAAT*TTTAGT*AT*A	DNA	Dig	—
U11(3-29)	IUIUICCAUCACIACAIAAICUUU(dC*) <sub>4</sub> dT	2'-OMe	Bio	Montzka-Wassarman and Steitz, 1992
U12(54-70)	UCUCACAUAICAIUIAII(dC*) <sub>4</sub> dT	2'-OMe	Bio	Montzka-Wassarman and Steitz, 1992
7SK(17-35)	(dC*) <sub>4</sub> CAIAUIUCICAICCA	2'-OMe	Bio	Wassarman and Steitz, 1991
7SK(209-223)	(dC*) <sub>4</sub> IAIIUUCUAICAIIG	2'-OMe	Bio	Wassarman and Steitz, 1991
7SK(220-240)	(dC*) <sub>4</sub> CCUUIAIAICUUIUUUIAII	2'-OMe	Bio	Wassarman and Steitz, 1991
EBER-1(13-28)	ICAAAACCUCUAIIC(dC*) <sub>4</sub> dA	2'-OMe	Bio	—
Poly T	TT(T*TTTT) <sub>7</sub> T*TT	DNA	Dig	—

B, Biotin phosphoramidite; C\*, amine modified Cytosine; T\*, amine modified Thymidine; Bio, Biotin; Dig, Digoxigenin; Flu, Fluorescein.

in CBs. Only upon double labeling of HeLa-ATCC cells with U1 and U2 probes (Fig. 3, *d-f*) was it apparent that U1 is detectable in coiled bodies, albeit at a lower intensity ratio to the nucleoplasm than with other snRNP probes (see below).

Several alternative probes for other snRNPs were also constructed. In Fig. 3 (*g-i*) the U6(81-101) and U2(30-43) signals are shown to colocalize in JS1000 cells. The U6(57-74) probe was less effective for detecting the CBs compared to the U6(81-101) oligomer (not shown). However, U6(57-74) is directed against the region of U6 which is known to base pair with U4 (Hashimoto and Steitz, 1984; Bringmann et al., 1984), and has been shown not to disrupt the U4/U6 coparticle in 2'-OMe depletion assays (Blencowe et al., 1989). When the U6(21-40) oligomer was used, the relative intensity was much greater than that of the other U6 oligoprobes and CBs were not visible (data not shown). This result is most likely due to crosshybridization with U1 (Blencowe et al., 1989).

Blencowe et al. (1989) also noticed an apparent non-reciprocal effect regarding antisense selection of the U4/U6 particle. The U6(57-74) oligomer efficiently selects both U4 and U6, while the U4(1-20) oligomer selects only U4, even

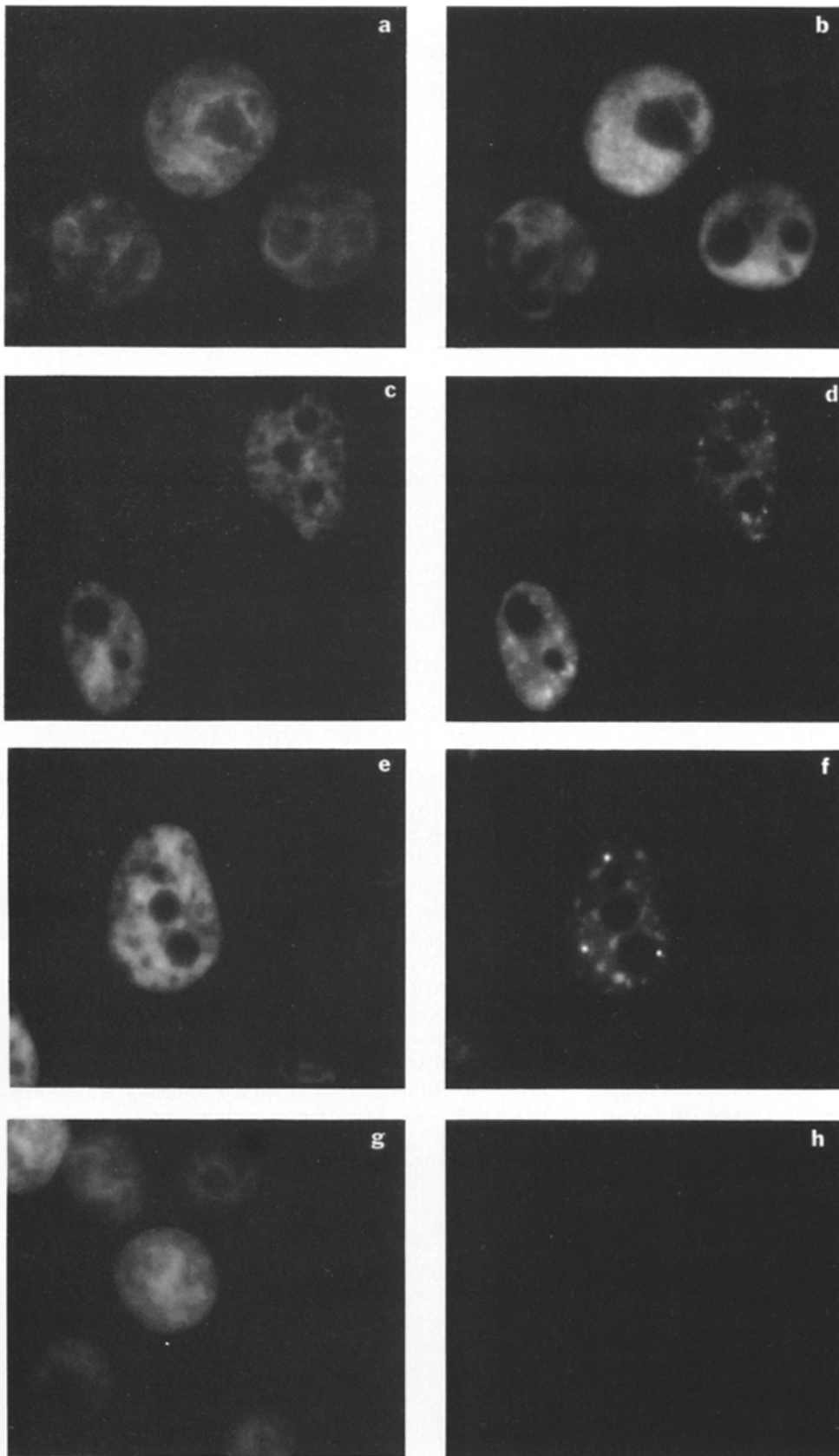
though it is also directed at the U4/U6 basepaired region. We also noted this nonreciprocal effect in experiments with the U4(1-20) probe, shown here in conjunction with the U2(25-43) oligomer (Fig. 3, *j-l*). As can be seen, U4 colocalizes with U2 in CBs. Interestingly, the U4(1-20) oligoprobe sometimes revealed additional ancillary structures not seen with any of the other antisense oligonucleotides. The doublet pattern of the ancillary spots shown in Fig. 3 *k* is particularly striking, especially in light of the findings of Ascoli and Maul (1991), who described several autoantisera that stain nuclear dots, some of which are also doublets (see Discussion).

The distribution of U5 was similar to that of U2 and U6 (data not shown). An oligomer complementary to the conserved loop of U5(U5[36-46]) was used. This probe is similar to that employed by Lamond et al. (Carmo-Fonseca et al., 1992), but does not contain 2'-aminoadenosine (see Table I).

#### Organization of U11, U12, and 7SK

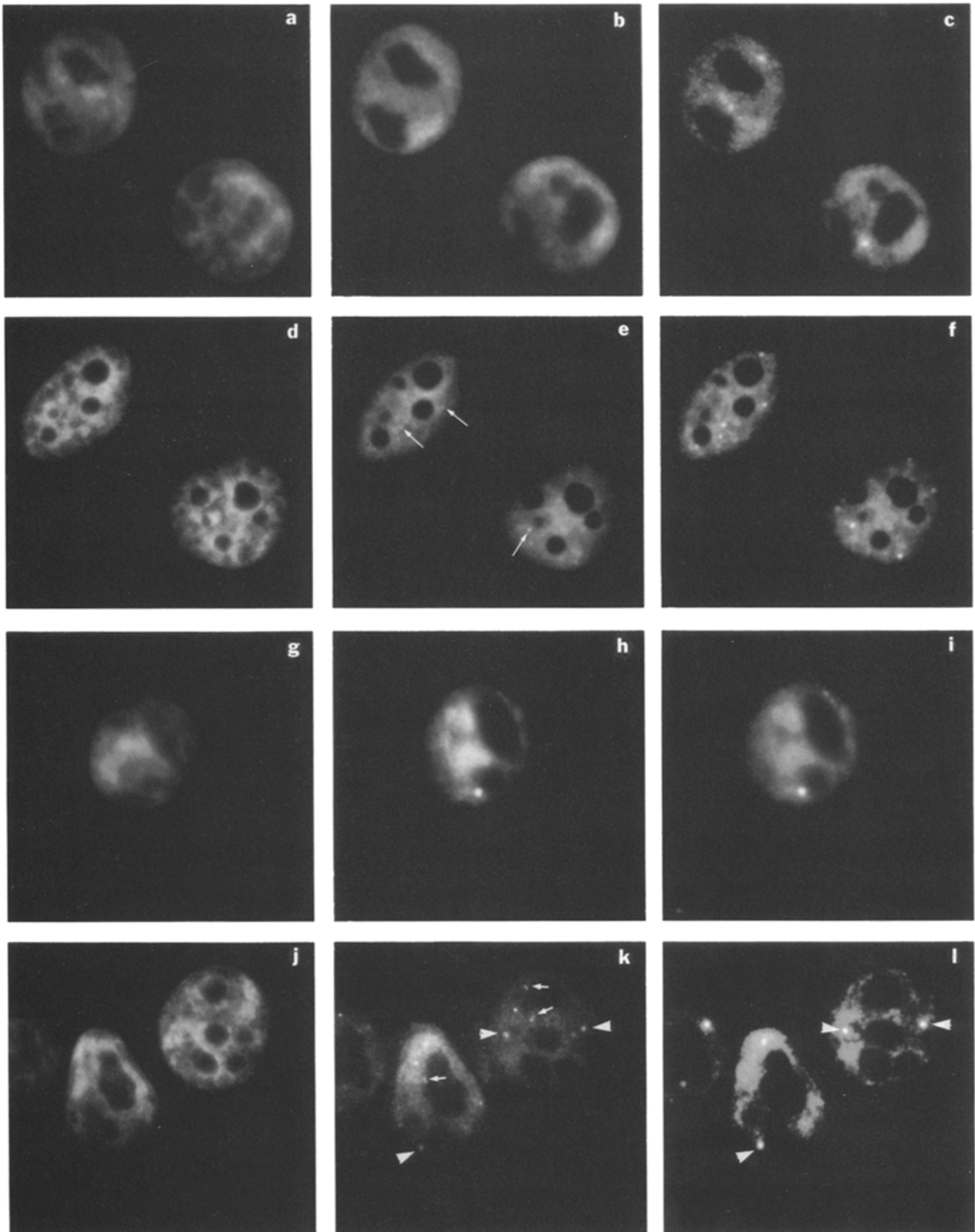
In addition to the spliceosomal snRNAs, we decided to investigate the organization of three less well-characterized snRNAs. Since the functions of U11, U12, and 7SK are presently unknown, their distribution within nuclei may pro-

Figure 1. Comparison of fixation conditions. A biotinylated 2'-OMe RNA antisense oligonucleotide U2(30-43) was hybridized to HeLa-JS1000 cells that were either preextracted with Triton X-100, and then fixed in paraformaldehyde (*a* and *b*; DAPI) or those which were fixed first, and then permeabilized with acetone (*c* and *d*). Cells fixed under the same conditions were also analyzed for the presence of the Sm protein using monoclonal antibody Y<sub>12</sub> (*e* and *f*-Triton; *g* and *h*-acetone; *e* and *g*-DAPI stain).



**Figure 2.** Comparison of the snRNP distributions in suspension (JS1000) and monolayer (ATCC) HeLa cells. Panels (a and b; DAPI, U1) reveal that U1(1-14) is widely distributed throughout the nucleoplasm of JS1000 cells, but coiled bodies were not observed. In ATCC cells (c and d—same as in a and b) the U1 signal is distributed in a speckled pattern throughout the nucleoplasm. Coiled bodies were also not readily detected. Panels (e and f; DAPI, U2) show that U2 is also organized in a speckled pattern in HeLa-ATCC cells (compare to Fig. 1, c and d) and CBs are easily detected. As a negative control (g and h; DAPI, EBER-1), an oligonucleotide complementary to an RNA produced by Epstein Barr Virus and known to be absent in HeLa-JS1000 cells shows only background hybridization throughout the nucleus and cytoplasm.





**Figure 3.** In situ colocalization of major snRNAs. Double labeling experiments were also performed in conjunction with anti-U2 oligomers. (*a-c*, HeLa-JS1000 cells; DAPI, U1, and U2). As shown, the U1(1-14) signals (*b*) colocalize with those of U2(25-43) (*c*), but U1 does not appear to concentrate in the CBs. (*d-f*, HeLa-ATCC cells; same as *a-c*) Double labeling of ATCC cells with anti-U1 oligomers (*e*) and an anti-U2 (*f*) probe (or anti-p80 coilin) reveals that U1 is present in CBs although the labeling is much weaker (*e*, *arrows*). (*g-i*; DAPI, U6, and U2) U6(81-101) (*h*) also colocalizes with U2(30-43) (*i*). (*j-l*; DAPI, U4, and U2) Interestingly, the U4(1-20) oligoprobe sometimes revealed additional ancillary structures not seen with any of the other antisense oligonucleotides. The U4 oligomer (*k*) reveals an interesting set of ancillary doublets (*arrows*) in addition to the more intense labeling of coiled bodies (*arrowheads*) also detected by the U2(25-43) probe (*l*).

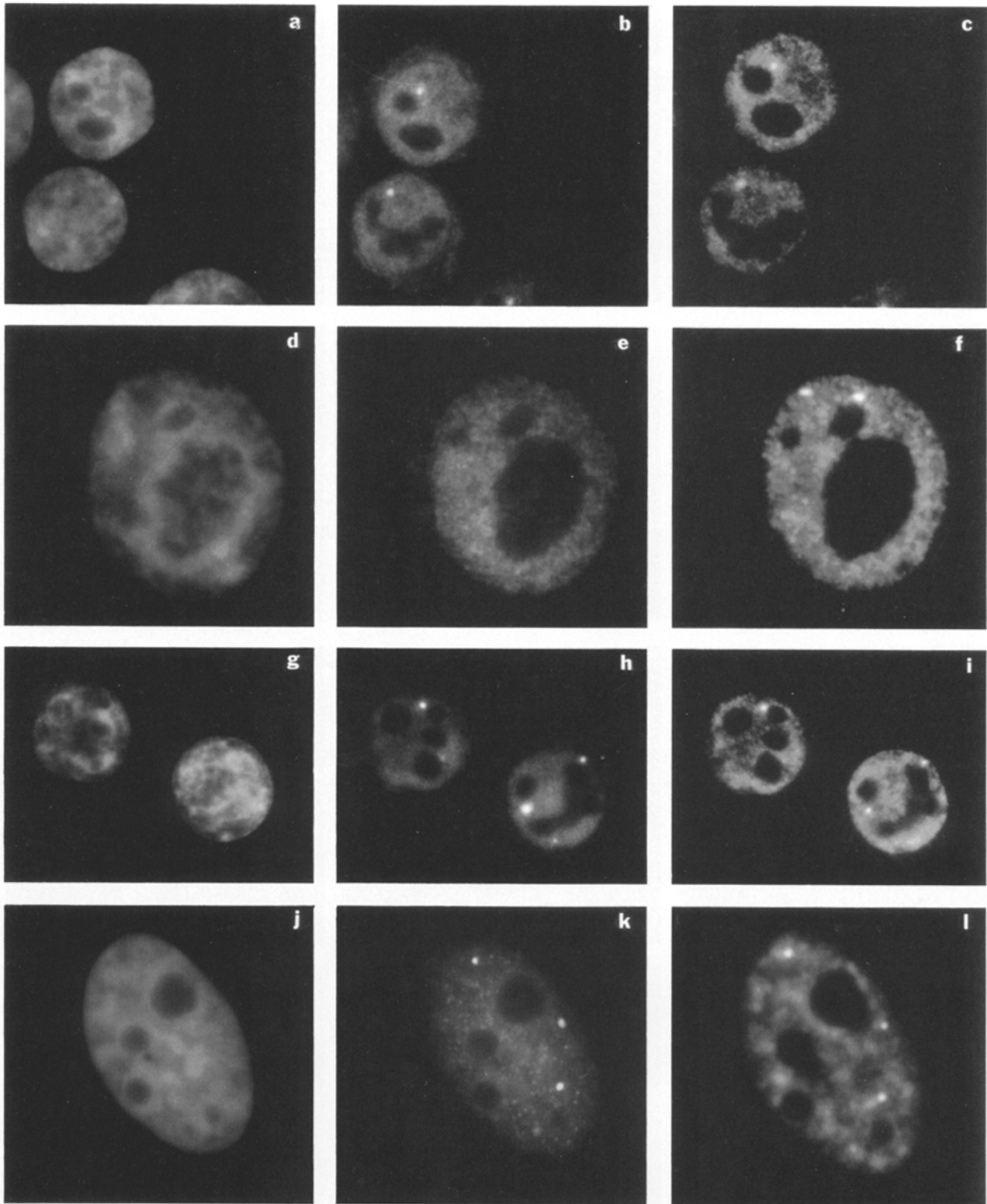


**Figure 4.** In situ colocalization of minor snRNAs and anti-snRNP antigens with U2. (*a-c*: JS-1000 cells; DAPI, U12, and U2) The U12(54–70) oligomer (*b*) also colocalizes with U2(25–43) (*c*). (*d-f*: JS-1000 cells; DAPI, 7SK, and U2) The 7SK snRNA, however, is found throughout the nucleoplasm but, like U1, it does not concentrate in the CBs. Two biotinylated 7SK oligomers (7SK[209–223] and 7SK[220–240]) (*e*) were used in conjunction with a digoxigenin-labeled U2(25–43) probe (*f*). Human autoimmune antisera specific for the U2 snRNPs were found to completely colocalize with antisense U2 oligomers. An example of this work is shown in (*g-i*: JS-1000 cells; DAPI, U2 RNA, and U2 protein) using the anti-U2(30–43) oligoprobe (*h*) and human autoimmune serum Ga (*i*). (*j-l*: ATCC cells; DAPI, U2, and p80 coilin) As a control, the bright foci detected with the U2(30–43) oligomer (*k*) colocalize with the anti-p80 coilin-positive CBs (*l*). The presence of less intense, diffuse nucleoplasmic signals suggests that some coilin protein is present in the nucleoplasm. Additional experiments with HeLa-JS1000 cells yielded equivalent results (not shown).



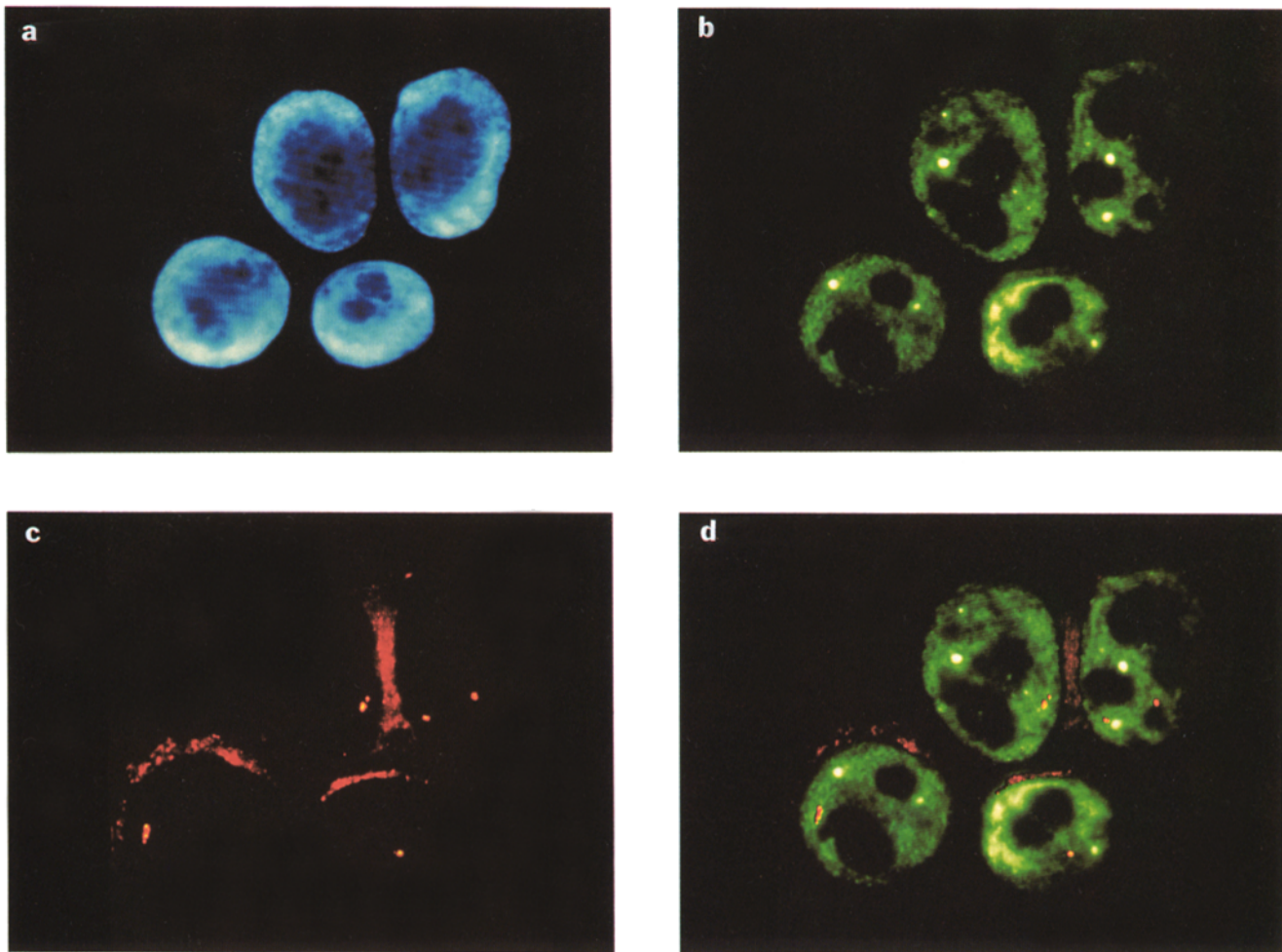


**Figure 5.** The snRNP-rich coiled bodies are not the sites of U2 transcription. A double label experiment involving sequential hybridization of a biotinylated U2(30–43) oligomer, followed by a digoxigenin-labeled U2 gene probe, revealed that the coiled bodies do not colocalize with the U2 genes on human chromosome 17. (a) DNA counterstain; (b) U2 snRNA oligoprobe alone; (c) U2 gene probe alone (the photo was intentionally overexposed to visualize the nuclear outline); and (d) merged images from b and c.

vide insight into possible mechanisms in which they might participate. Fig. 4 (a–c) shows that the U12 and U2 snRNPs colocalize, while Fig. 4 (d–f) reveals that 7SK is widely dispersed throughout the nucleoplasm but is not concentrated in the CBs. All three of the 7SK oligoprobes (Table I) gave equivalent results. Two different biotinylated 7SK probes (7SK[209–223] and 7SK[220–240], Fig. 4 e) were used in conjunction with the digoxigenin-labeled U2(25–43) oligomer to increase signal output. An oligonucleotide complementary to the 5' end of U11 (see Table I) was used in both single and double labeling experiments. As expected, the hybridization pattern of the U11(3–29) oligomer resembled that of the U12(54–70) probe (data not shown). However, this oligonucleotide brings down a substantial amount of U2 in particle selection assays (Montzka Wassarman and Steitz, 1992). Thus the pattern detected might be due to crosshybridization with U2 even though the washing stringency used here is substantially higher than that used to select snRNPs from cell extracts (700 mM Na, 42°C vs 250 mM Na, 0°C). The signals derived from the U12, U11, and 7SK snRNAs were visible by eye through the microscope, but were relatively weak. Structural details that were not readily visible by eye were easily detected by the CCD camera. Hence, the double

labeling procedure described here allowed efficient discrimination between probes that concentrated in CBs and those that did not.

#### ***Antisense snRNA Probes Colocalize with snRNP Protein and CB Antibodies***

Using human autoimmune antisera known to be specific for the U2 (serum Ga or Ya) or U1 (serum Do) snRNPs in combination with their respective oligonucleotide probes, the snRNP antigens were found to completely colocalize with the snRNAs themselves. An example of this work using biotinylated anti-U2(30–43) and anti-U2 serum Ga is shown in Fig. 4 (g–i). Additional experiments performed on HEp-2 cells using an antinuclear antibody immunofluorescence assay kit (see Materials and Methods) revealed a speckled pattern in addition to less intense, widespread nucleoplasmic staining (not shown). As a control for coiled bodies, the anti-p80 coilin antibody (Andrade et al., 1991; Andrade et al., 1993) was used in conjunction with the U2(25–43) oligomer (Fig. 4, j–l). These observations confirm that the snRNP-rich structures (seen in Fig. 4 l) colocalize with the p80 coilin-positive CBs (Fig. 4 k).

### The snRNP-Rich Coiled Bodies Are Not the Sites of U2 Transcription

Carmo-Fonseca et al. (1992) have recently shown that snRNPs no longer concentrate in CBs upon heat shock at 45°C or after treatment with transcriptional inhibitors such as  $\alpha$ -amanitin or actinomycin D. We have confirmed that heat shock at 45°C disrupts the association of the U2 snRNP with CBs in MCF-7 cells (Vourch, C., and A. G. Matera, unpublished observations). Heat shock at 45°C and recovery at 37°C or heat shock at 42°C without recovery did not eliminate the CBs. These striking results suggest a link between CBs and transcription (Carmo-Fonseca et al., 1992). A possible explanation for this connection is that (in analogy to rDNA and nucleoli) coiled bodies are indeed the site(s) of higher order snRNP assembly and may therefore also be the site(s) of snRNA transcription. The colocalization of snRNP proteins, which are thought to be acquired in the cytoplasm (for review see Izaurralde and Mattaj, 1992), and snRNAs within the CBs suggests that assembled snRNP particles are being detected. Previous investigators have described specific loci within amphibian lampbrush chromosomes called sphere organizer regions (Callan, 1986; Callan et al., 1991). Thus if coiled bodies were a kind of snRNP nucleolus, the snRNA genes should also colocalize with the CBs. To test this hypothesis, a double label experiment involving sequential hybridization of a biotinylated probe for the U2 snRNAs, followed by a digoxigenin-labeled U2 gene probe, revealed that CBs do not colocalize with the U2 genes (Fig. 5). Thus, coiled bodies are not the sites of U2 transcription. RNase digestion disrupts CBs, while DNase does not (Carmo-Fonseca et al., 1991b). However, such experiments give no information regarding the relative location of specific DNA loci. Since the other spliceosomal snRNAs are present in CBs, it is also unlikely that transcription of other snRNA genes occurs in CBs.

### Most of the U2 snRNP Is Located in the Nucleoplasm, Not in Coiled Bodies

The initial experiments of Lamond et al. (Carmo-Fonseca et al., 1991b) showed that mammalian nuclei contain coiled bodies which are highly enriched in snRNPs. Images obtained with confocal microscopes are very useful for assaying relative intensities within a particular optical section. However, wide field epifluorescence imaging systems are more appropriate for two dimensional quantification, since a larger fraction of the cellular volume can be compared. To quantify the extent to which snRNPs are concentrated in the CBs, we measured and compared the relative fluorescent intensities of the signals from the CBs, nucleoplasm, and background in both JS1000 and ATCC HeLa cells. The results of this comparison are shown in Table II. The intensity values (essentially a photon count) for the background and nucleoplasm were determined by using a histogram of the data from a defined area for each of 30 sample nuclei. Examples of these plots are illustrated in Fig. 6. The intensity values recorded by the CCD camera are plotted against the number of pixels having that intensity. The peak of the distribution for each cell analyzed was used to compute the average intensities of the nucleoplasm and background shown in Table II. For a 5-s exposure, the average intensity of the nucleoplasm in JS1000 cells was 921 U/pixel and that of the background was 278, while the nucleoplasm in ATCC cells measured 705

Table II. Quantitative Analysis of U2 snRNA

Location	Signal Intensity*			
	U2(30-43)		EBER-1 JS1000	Mock JS1000
	JS1000	ATCC		
Background	278	286	274	272
Nucleoplasm	921	705	360	308
Coiled bodies	2863	2428	—	—
Intensity ratio of coiled bodies/nucleoplasm†	4.02	5.11		
Average number of coiled bodies per nucleus	1.71‡	3.72‡		

\* Average intensity value for a 5-s exposure. 30 nuclei counted.

† After subtraction of background value. Ratio was essentially constant over 50-s exposure.

‡ For HeLa-JS1000 cells, calculated from a sample of 95 nuclei.  $\sigma = 0.89$

§ Carmo-Fonseca et al., 1991b.

U/pixel and the background was 286 (see Table II). The nucleoplasm in the control experiments measured 360 U/pixel for the heterologous (EBER-1) oligomer and 308 U/pixel for a mock hybridization without a biotinylated probe. Because of the relatively small size of the CBs, and the somewhat arbitrary boundaries of these structures, the maximum intensity value within each coiled body was used. The average value for JS1000 CBs was 2,863 U/pixel and that of ATCC cells was 2,428. After subtraction of the background values, the intensity ratio of coiled bodies to nucleoplasm was 4.02 for JS1000 cells and 5.11 for ATCC cells (see Table II). Since the maximum values were used to calculate the average CB intensity, this ratio represents an upper limit of the actual value. However, the nucleoplasm represents a much larger fraction of the cell volume (>100-fold) than the CBs. Therefore, the bulk of the U2 snRNP is located in the nucleoplasm. Also in Table II, we measured the average number of CBs per HeLa JS1000 cell from a sample of 95 nuclei. In contrast with the 3-4 CBs per monolayer HeLa cell observed by Carmo-Fonseca et al. (1991b), only 1-2 were detected in the JS1000 cells.

### Discussion

Elucidation of the functional diversity of the mammalian nucleus has been hampered by its apparent structural homogeneity. The lack of membranous organelles in the nucleus makes fractionation and localization of functional domains difficult. However, recent immunofluorescence studies of amphibian oocytes reveal the existence of several extrachromosomal nuclear organelles which contain snRNPs (Wu et al., 1991; Callan and Gall, 1991). In this study, we investigate the distribution of major and minor snRNAs within HeLa cell nuclei. Our results show that each of the U1, U2, U4, U5, U6, U11, U12, and 7SK snRNPs are widely distributed throughout the nucleoplasm, excluding nucleoli. In addition, the U2, U4, U5, U6, U11, and U12 snRNAs are enriched in CBs. Double labeling experiments with U2 antisense probes reveal that the U1 and 7SK snRNAs colocalize, but do not concentrate in the CBs. This difference in the distribution of U1 and U2 RNAs has also been observed by Lamond et al. in mammalian cells (Carmo-Fonseca et al., 1991a,b, 1992) as well as by Gall et al. in amphibian oocytes (Wu et al., 1991; Callan and Gall, 1991).

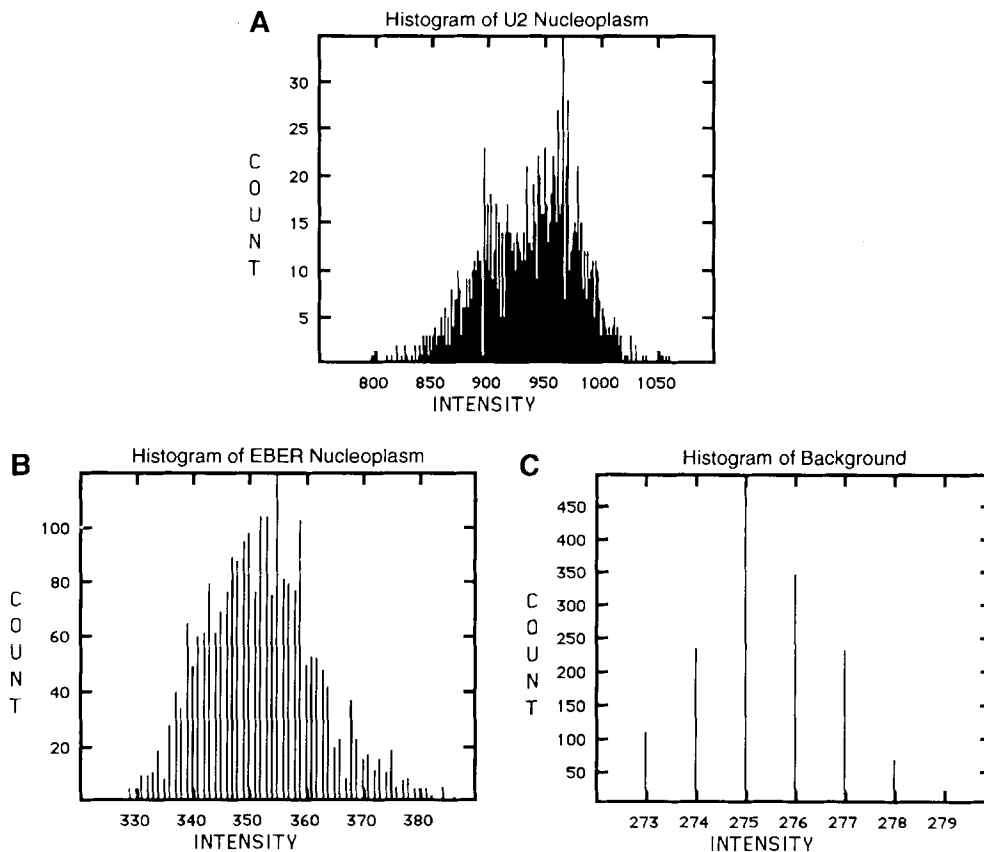


**Figure 6.** Most of the U2 snRNP is located in the nucleoplasm, not in coiled bodies. Data from HeLa-JS1000 cell sample images used in the calculation of the results in Table II are shown above. In *A* and *B* the fluorescent intensities from the nucleoplasm when hybridized with U2(30–43) and EBER-1(13–28), respectively, are displayed. A total of 30 such distributions were calculated, one for each nucleus examined. The peak of each distribution was recorded for use in calculating the average intensities listed in Table II. In *C*, the noncellular background noise was measured. In the examples above, the intensity value used for *A* was 962, *B* was 350, and that for *C* was 275.

### Transcription and Splicing

In contrast with the progress that has been made in analyzing the splicing machinery *in vitro*, relatively little is known about how splicing factors are organized *in vivo* or how splicing is integrated with transcription, polyadenylation, and transport. The widespread nucleoplasmic organization of the spliceosomal snRNPs seen in this study argues that pre-mRNA splicing takes place in the nucleoplasm. Furthermore, quantitation of the intracellular distribution of the U2 snRNP supports this view. Since most of the U2 RNA is located in the nucleoplasm, it is reasonable to assume that splicing begins at or near the DNA template, not in coiled bodies. The very similar distributions of additional pre-mRNA processing factors such as U2AF (Zamore and Green, 1991; Carmo-Fonseca et al., 1991b) and several classes of hnRNP (Choi and Dreyfuss, 1984; Piñol-Roma et al., 1989; Carmo-Fonseca et al., 1991a) also support this interpretation.

Our results show that antibody probes specific for the U1 and U2 snRNPs completely colocalize with their respective antisense snRNA counterparts. We have also demonstrated that the precise nature of the nucleoplasmic distribution of snRNPs can differ, depending on cell type. Two different strains of HeLa cells, one which grows in suspension (HeLa-JS1000) and the other in monolayers (HeLa-ATCC), show varying degrees of speckling throughout the nucleoplasm (compare Figs. 1*d* and 2*f*). Even after allowing JS1000 cells to grow adherently, speckles were not apparent. Metabolism in general and transcription of mRNA in particular are dynamic processes. Thus the amount of snRNA detected within nucleoplasmic speckles (and coiled bodies) may change in response to growth conditions or other physiological stimuli.

If splicing is in fact initiated near the DNA template, the nuclear distribution of poly(A) RNA should be similar to that of the spliceosomal snRNPs. Carter et al. (1991) have shown that poly(A) RNA is also organized in a speckled pattern throughout the nucleoplasm. In acetone permeabilized HeLa-ATCC cells, we found that the nucleoplasmic speckles seen with the biotinylated U2(30–43) probe indeed colocalized with a digoxigenin-labeled poly(T) oligomer, although there was also a substantial labeling of the cytoplasm with the poly(T) probe (Matera, A. G., unpublished observations, see also Taneja et al., 1992). Poly(A) RNA was not found to be concentrated in the CBs.

### Coiled Bodies

If CBs are not the actual sites of pre-mRNA splicing, what then is their function? Our results confirm that the snRNP-rich nuclear foci colocalize with anti-p80 coilin antibodies (Fig. 4, *j-l*). This colocalization has been shown to be dependent upon transcription and is disrupted by heat shock (Carmo-Fonseca et al., 1992). Furthermore, we demonstrate that CBs do not colocalize with the U2 genes and thus are not the sites of U2 snRNA transcription (Fig. 5).

Psoralen crosslinking studies *in vitro* indicate that U1 is the first snRNP to bind to pre-mRNA (before U2, U4, U5, and U6) and perhaps the first to be released (Wassarman and Steitz, 1992). Additional cross-linking experiments reveal that U6 can simultaneously interact with U2 and U4. Taken together with the evidence that U5 can also associate with U4/U6 to form a tri-snRNP, it seems possible that U2/U4/U5/U6 could join the splicing reaction as a pre-formed complex *in vivo* after U1 binds (Wassarman and

Steitz, 1992). In fact, a U2/U4/U5/U6 pseudospliceosome particle has been detected in the absence of pre-mRNA in vitro (Konarska and Sharp, 1988). Thus, these data are consistent with the hypothesis that CBs represent sites of multi-particle snRNP assembly.

It has also been postulated that CBs might participate in some form of snRNP recycling, intron debranching, or degradation activity and thereby be detected due to an accumulation of postsplicing components (Carmo-Fonseca et al., 1992). However, snRNP assembly and recycling/transport are not necessarily mutually exclusive processes, and could likely be carried out in the same cellular locale. Regarding snRNP recycling/transport, it is noteworthy that U2, U11, and U12 share a similar distribution pattern. The function(s) of the U11 and U12 snRNAs are unknown, although U11 and U12 have been shown to comprise a coparticle (Montzka Wassarman and Steitz, 1992). Beemon et al. have recently described a negative regulator of splicing (NRS) that may be involved in the accumulation of unspliced RNA in RSV transfected cells (McNally et al., 1991; McNally and Beemon, 1992). This NRS was recently found to inhibit splicing in vitro and bind U1, U2, U11, and U12 (Gontarek, R. R., and K. Beemon, personal communication), prompting speculation that U11/U12 might somehow be involved in regulating splicing and/or polyadenylation. However, it is possible that U11/U12 are involved in intron degradation and/or mRNA transport of normal cellular messages and that RSV has evolved a mechanism to evade splicing. In this scenario, U1 would not be part of the preassembled splicing complexes (U2/U4/U5/U6), but it would be part of the putative recycling/mRNA transport machinery (U1/U2/U11/U12). Of particular note, is the fact that U1 appears to be less concentrated in CBs than the other spliceosomal snRNPs and more concentrated in the nucleoplasm (see Fig. 3, a-c).

### 7SK Interactions

The distributions of U1 and 7SK are also similar, although we see no evidence of 7SK in CBs. Speculation on possible functions of 7SK RNPs are numerous, including a possible base pairing interaction with U4 (Wassarman and Steitz, 1991). This putative interaction might reasonably take place after melting of the U4/U6 particle during the second step of splicing (Lamond et al., 1988). However, the absence of 7SK and the presence of U4 within CBs argues that this putative U4/7SK interaction would take place in the nucleoplasm, again consistent with CBs participating in some postsplicing, snRNP reassembly event. Interestingly, U4 was sometimes detected in additional, less intense foci that do not contain U2. These ancillary structures sometimes appeared as doublets. Ascoli and Maul (1991) have recently identified human antisera which stain the nucleoplasm in a punctate manner involving large and small (sometimes doublet) nuclear dots. Affinity purified antibodies to a common 55-kD antigen stained foci-like structures exclusively. Perhaps this 55-kD protein is an additional component of CBs which is also associated with some aspect of U4 metabolism. Interestingly, there is a ~52-kD protein initially associated with U5 that is phosphorylated exclusively in U4/5/6 tri-snRNPs and cannot be detected in purified spliceosomes (Behrens and Lührmann, 1991). Future studies may elucidate possible interactions of this protein with U4.

### Technical Issues

One of the major concerns of previous studies (Carmo-Fonseca et al., 1991a,b) was that antibody and antisense probes for the U2 snRNP did not entirely colocalize. Only after a low salt/EDTA/SDS extraction procedure did the nucleoplasmic U2 antisense RNA binding sites become unmasked (Carmo-Fonseca et al., 1992). Although lipid extraction is crucial for detector permeability, the authors do not mention possible effects that low salt and chelators might have on this unmasking process. In addition, Carmo-Fonseca et al. (1991b, cf. Fig. 6 F) have also shown that preextracted nuclei from HeLa cells grown in suspension do in fact reveal a significant amount of nucleoplasmic U2 signal. Furthermore, Huang and Spector (1992) noted that, in their hands, extended hybridization times were required to observe significant nucleoplasmic hybridization. We detected no such kinetic effect. It is important to note that both of the above studies used monolayer HeLa cells and hybridization stringencies ~20°C lower than those used here. While it is possible that antisense RNA binding sites might be unavailable at the lower hybridization temperatures, perhaps the observed differences in labeling reflect some inherent change in the metabolic (i.e., transcriptional) activity of the cells themselves. Thus, coiled bodies might only be visible in cells which are actively engaged in transcription of pre-mRNAs, thus requiring the assembly of a large number of snRNP complexes. Indeed, Spector et al. (1992) have shown that coiled bodies are more frequently observed in highly transformed cell lines. Furthermore, they found that CBs are not readily detected in nonimmortalized cells. A particularly slow step in the kinetics of spliceosome formation might reasonably be the preassembly of a U2/U4/U5/U6 particle. Thus, the steady state amount of snRNPs in coiled bodies may change in response to the needs of the cell in terms of its overall transcriptional activity.

We are deeply indebted to Dr. J. Steitz and the members of her laboratory for sharing reagents, protocols, and ideas. We are grateful to E. Chan and E. Tan for providing the anti-p80 coilin antibodies, and to S. Wolin and A. Helenius for the HeLa-ATCC cell line. We also thank J. Steitz, A. Weiner, D. Wassarman, K. Tyc, S. Baserga, E. Sontheimer, K. Wassarman, D. Toczyski, and C. Vourc'h for helpful discussions and critical reading of the manuscript.

A. G. Matera was supported by a Damon Runyon-Walter Winchell Cancer Research Fund postdoctoral fellowship, DRG-1135. This work was supported by U.S. Public Health Service grants HG-00246 and GM-40115.

Received for publication 6 August 1992 and in revised form 21 January 1993.

### References

- Andrade, L. E. C., E. K. L. Chan, I. Raska, C. L. Peebles, G. Roos, and E. M. Tan. 1991. Human autoantibody to a novel protein of the nuclear coiled body: immunological characterization and cDNA cloning of p80-coilin. *J. Exp. Med.* 173:1407-1419.
- Andrade, L. E. C., E. M. Tan, and E. K. L. Chan. 1993. Immunocytochemical analysis of the coiled body in the cell cycle and during cell proliferation. *Proc. Natl. Acad. Sci. USA.* 90:1947-1951.
- Ascoli, C. A., and G. G. Maul. 1991. Identification of a novel nuclear domain. *J. Cell Biol.* 112:785-795.
- Bacallao, R., M. Bomsel, E. H. K. Stelzer, and J. de May. 1989. Guiding principles of specimen preservation for confocal fluorescent microscopy. In *Handbook of Biological Confocal Microscopy*. J. Pawley, editor. IMR Press, Madison. 181-187.
- Behrens, S.-E., and R. Lührmann. 1991. Immunoaffinity purification of a [U4/U6.U5] tri-snRNP from human cells. *Genes & Dev.* 5:1439-1452.

- Blencowe, B. J., B. S. Sproat, U. Ryder, S. Barabino, and A. I. Lamond. 1989. Antisense probing of the human U4/U6 snRNP with biotinylated 2'-Ome RNA oligonucleotides. *Cell* 59:531-539.
- Bringmann, P., B. Appel, J. Rinke, R. Reuter, and R. Lührmann. 1984. Evidence for the existence of snRNAs U4 and U6 in a single ribonucleoprotein complex and for their association by intermolecular base pairing. *EMBO (Eur. Mol. Biol. Organ.) J.* 3:1357-1363.
- Brown, A. M. C., J. M. Jeltsch, M. Roberts, and P. Chambon. 1984. Activation of pS2 gene transcription is a primary response to estrogen in the human breast cancer cell line MCF-7. *Proc. Natl. Acad. Sci. USA* 81:6344-6348.
- Bruzik, J. P., and J. A. Steitz. 1990. Spliced leader RNA sequences can substitute for the essential 5' end of U1 RNA during splicing in a mammalian in vitro system. *Cell* 62:889-899.
- Callan, H. G. 1986. *Lampbrush Chromosomes*. Springer-Verlag, Berlin/New York. 1-254.
- Callan, H. G., and J. G. Gall. 1991. Association of RNA with the B and C snurposomes of *Xenopus* oocyte nuclei. *Chromosoma (Berl.)* 101:69-82.
- Callan, H. G., J. G. Gall, and C. Murphy. 1991. Histone genes are located at the sphere loci of *Xenopus* lampbrush chromosomes. *Chromosoma (Berl.)* 101:245-251.
- Carmo-Fonseca, M., R. Pepperkok, B. S. Sproat, W. Ansorge, M. S. Swanson, and A. I. Lamond. 1991a. In vivo detection of snRNP-rich organelles in the nuclei of mammalian cells. *EMBO (Eur. Mol. Biol. Organ.) J.* 10:1863-1873.
- Carmo-Fonseca, M., D. Tollervey, R. Pepperkok, S. M. L. Barabino, A. Merdes, C. Brunner, P. D. Zamore, M. R. Green, E. Hurt, and A. I. Lamond. 1991b. Mammalian nuclei contain foci which are highly enriched in components of the pre-mRNA splicing machinery. *EMBO (Eur. Mol. Biol. Organ.) J.* 10:195-206.
- Carmo-Fonseca, M., R. Pepperkok, M. T. Carvalho, and A. I. Lamond. 1992. Transcription-dependent colocalization of the U1, U2, U4/U6, and U5 snRNPs in coiled bodies. *J. Cell Biol.* 117:1-14.
- Carter, K. C., K. L. Taneja, and J. B. Lawrence. 1991. Discrete nuclear domains of poly(A) RNA and their relationship to the functional organization of the nucleus. *J. Cell Biol.* 115:1191-1202.
- Choi, Y. D., and G. Dreyfuss. 1984. Monoclonal antibody characterization of the C proteins of heterogeneous nuclear ribonucleoprotein complexes in vertebrate cells. *J. Cell Biol.* 99:1997-2004.
- Craft, J., T. Mimori, T. L. Olsen, and J. A. Hardin. 1988. The U2 small nuclear ribonucleoprotein particle as an autoantigen: analysis with sera from patients with overlap syndromes. *J. Clin. Invest.* 81:1716-1724.
- Elicieri, G. L., and J. S. Ryerse. 1984. Detection of intranuclear clusters of Sm antigens with monoclonal anti-Sm antibodies by immunoelectron microscopy. *J. Cell Physiol.* 121:449-451.
- Fakan, S., G. Leser, and T. E. Martin. 1984. Ultrastructural distribution of nuclear ribonucleoproteins as visualized by immunocytochemistry on thin sections. *J. Cell Biol.* 98:358-363.
- Gall, J. G. 1991. Spliceosomes and snurposomes. *Science (Wash. DC)* 252:1499-1500.
- Gall, J. G., and H. G. Callan. 1989. The sphere organelle contains small nuclear ribonucleoproteins. *Proc. Natl. Acad. Sci. USA* 86:6635-6639.
- Green, M. R. 1991. Biochemical mechanisms of constitutive and regulated pre-mRNA splicing. *Annu. Rev. Cell Biol.* 7:559-599.
- Guthrie, C. 1991. Messenger RNA splicing in yeast: clues to why the spliceosome is a ribonucleoprotein. *Science (Wash. DC)* 253:157-163.
- Hardin, J. H., S. S. Spicer, and W. B. Greene. 1969. The paranuclear structure, accessory body of Cajal, sex chromatin and related structures in nuclei of rat trigeminal neurons: a cytochemical and ultrastructural study. *Anat. Rec.* 164:403-432.
- Hashimoto, C., and J. A. Steitz. 1984. U4 and U6 RNAs co-exist in a single small nuclear ribonucleoprotein particle. *Nucl. Acids Res.* 12:3283-3293.
- Huang, S., and D. L. Spector. 1992. U1 and U2 small nuclear RNAs are present in nuclear speckles. *Proc. Natl. Acad. Sci. USA* 89:305-308.
- Iyer, R. P., W. Egan, J. B. Regan, and S. L. Beaucage. 1990. 3H-1,2-Benzodithiole-3-one 1,1-dioxide as an improved sulfurizing reagent in the solid-phase synthesis of oligodeoxyribonucleoside phosphorothioates. *J. Am. Chem. Soc.* 112:1253-1254.
- Izaurralde, E., and I. W. Mattaj. 1992. Transport of RNA between nucleus and cytoplasm. *Sem. Cell Biol.* 3:279-288.
- Konarska, M. M., and P. A. Sharp. 1988. Association of U2, U4, U5, and U6 small nuclear ribonucleoproteins in a spliceosome-type complex in absence of precursor RNA. *Proc. Natl. Acad. Sci. USA* 85:5459-5462.
- Lafarga, M., J. P. Hervas, M. C. Santa-Cruz, J. Villegas, and D. Crespo. 1983. The "accessory body" of Cajal in the neuronal nucleus: a light and electron microscopic approach. *Anat. Embryol.* 166:19-30.
- Lamond, A. I., M. M. Konarska, P. J. Grabowski, and P. A. Sharp. 1988. Spliceosome assembly involves binding and release of U4 small nuclear ribonucleoprotein. *Proc. Natl. Acad. Sci. USA* 85:411-415.
- Lerner, E. A., M. R. Lerner, C. A. Janeway, and J. A. Steitz. 1981. Monoclonal antibodies to nucleic acid-containing cellular constituents: probes for molecular biology and autoimmune disease. *Proc. Natl. Acad. Sci. USA* 78:2737-2741.
- Leser, G. P., S. Fakan, and T. E. Martin. 1989. Ultrastructural distribution of ribonucleoprotein complexes during mitosis: snRNP antigens are contained in mitotic granule clusters. *Eur. J. Cell Biol.* 50:376-389.
- Lichter, P., C.-j. C. Tang, K. Call, G. Hermanson, G. A. Evans, D. Housman, and D. C. Ward. 1990. High resolution mapping of human chromosome 11 by *in situ* hybridization with cosmid clones. *Science (Wash. DC)* 247:64-69.
- Matera, A. G., and D. C. Ward. 1992. Oligonucleotide probes for the analysis of specific repetitive DNA sequences by fluorescence *in situ* hybridization. *Human Molecular Genetics* 1:535-539.
- McNally, M. T., and K. Beemon. 1992. Intronic sequences and 3' splice sites control Rous sarcoma virus RNA splicing. *J. Virol.* 66:6-11.
- McNally, M. T., R. R. Gontarek, and K. Beemon. 1991. Characterization of Rous sarcoma virus intronic sequences that negatively regulate splicing. *Virology* 185:99-108.
- Monneron, A., and W. Bernhard. 1969. Fine structural organization of the interphase nucleus in some mammalian cells. *J. Ultrastruct. Res.* 27:266-288.
- Montzka Wassarman, K., and J. A. Steitz. 1992. The low-abundance U11 and U12 small nuclear ribonucleoproteins (snRNPs) interact to form a two-snRNP complex. *Mol. Cell Biol.* 12:1276-1285.
- Nyman, U., H. Hallman, G. Hadlaczy, I. Pettersson, G. Sharp, and N. R. Ringertz. 1986. Intranuclear localization of snRNP antigens. *J. Cell Biol.* 102:137-144.
- Piñol-Roma, S., M. S. Swanson, J. G. Gall, and G. Dreyfuss. 1989. A novel heterogeneous nuclear RNP protein with a unique distribution on nascent transcripts. *J. Cell Biol.* 109:2575-2587.
- Ramon y Cajal, S. R. 1903. Un sencillo metodo de coloracion selectiva del reticulo protoplasmico y sus efectos en los diversos organos nerviosos de vertebrados y invertebrados. *Trab. Lab. Invest. Biol. (Madrid)* 2:129-221.
- Raska, I., R. L. Ochs, L. E. C. Andrade, E. K. L. Chan, R. Burlingame, C. Peebles, D. Gruol, and E. M. Tan. 1990. Association between the nucleolus and the coiled body. *J. Struct. Biol.* 104:120-127.
- Raska, I., L. E. C. Andrade, R. L. Ochs, E. K. L. Chan, C.-M. Chang, G. Roos, and E. M. Tan. 1991. Immunological and ultrastructural studies of the nuclear coiled body with autoimmune antibodies. *Exp. Cell Res.* 195:27-37.
- Reddy, R., and H. Busch. 1988. Small nuclear RNAs: RNA sequences, structure and modifications. In *Structure and Function of Major and Minor Small Nuclear Ribonucleoproteins*. M. L. Birnstiel, editor. Springer-Verlag, Berlin/New York. 1-37.
- Seite, R., M. J. Pebusque, and M. Vio-Cigna. 1982. Argrophilic proteins on coiled bodies in sympathetic neurons identified by Ag-NOR procedure. *Biol. Cell* 46:97-100.
- Spector, D. L. 1984. Colocalization of U1 and U2 small nuclear RNPs by immunocytochemistry. *Biol. Cell* 51:109-112.
- Spector, D. L. 1990. Higher order nuclear organization: three-dimensional distribution of small nuclear ribonucleoprotein particles. *Proc. Natl. Acad. Sci. USA* 87:147-151.
- Spector, D. L., G. Lark, and S. Huang. 1992. Differences in snRNP localization between transformed and nontransformed cells. *Mol. Biol. Cell* 3:555-569.
- Steitz, J. A., D. L. Black, V. Gerke, K. A. Parker, A. Kramer, D. Frendewey, and W. Keller. 1988. Functions of the abundant U-snRNPs. In *Structure and Function of Major and Minor Small Nuclear Ribonucleoproteins*. M. L. Birnstiel, editor. Springer-Verlag, Berlin/New York. 115-154.
- Taneja, K. L., L. M. Lifshitz, F. S. Fay, and R. H. Singer. 1992. Poly(A) RNA codistribution with microfilaments: evaluation by *in situ* hybridization and quantitative digital imaging microscopy. *J. Cell Biol.* 119:1245-1260.
- Toczyski, D. P. W., and J. A. Steitz. 1991. EAP, a highly conserved cellular protein associated with Epstein-Barr virus small RNAs (EBERs). *EMBO (Eur. Mol. Biol. Organ.) J.* 10:459-468.
- Verheijen, R., H. Kuijpers, P. Vooijs, W. van Venrooij, and F. Ramaekers. 1986. Distribution of the 70k U1 RNA-associated protein during interphase and mitosis: correlation with other U RNP particles and proteins of the nuclear matrix. *J. Cell Sci.* 86:173-190.
- Wassarman, D. A., and J. A. Steitz. 1991. Structural analyses of the 7SK ribonucleoprotein (RNP), the most abundant human small RNP of unknown function. *Mol. Cell Biol.* 11:3432-3445.
- Wassarman, D. A., and J. A. Steitz. 1992. Psoralen crosslinking detects specific interactions of U1, U2, U5 and U6 small nuclear RNAs with precursor messenger RNA during *in vitro* splicing. *Science (Wash. DC)* 257:1918-1925.
- Wu, Z., C. Murphy, H. G. Callan, and J. G. Gall. 1991. Small nuclear ribonucleoproteins and heterogeneous nuclear ribonucleoproteins in the amphibian germinal vesicle: loops, spheres and snurposomes. *J. Cell Biol.* 113:465-483.
- Zamore, P. D., and M. R. Green. 1991. Biochemical characterization of U2 snRNP auxiliary factor: an essential pre-mRNA splicing factor with a novel intranuclear distribution. *EMBO (Eur. Mol. Biol. Organ.) J.* 10:207-214.